

Application of white-beam X-ray microdiffraction for the study of mineralogical phase identification in ancient Egyptian pigments

P. A. Lynch,^{a,c*} N. Tamura,^b D. Lau,^a I. Madsen,^c D. Liang,^a M. Strohschneider^d and A. W. Stevenson^a

^aCSIRO MMT, Gate 5 Normanby Rd, Clayton, Victoria 3168, Australia, ^bLawrence Berkeley National Laboratory, 1 Cyclotron Road, Berkeley, CA 94720, USA, ^cCSIRO Minerals, Box 312, Clayton South, Victoria 3169, Australia, and ^dNational Gallery of Victoria, PO Box 7259, 180 St Kilda Road, Melbourne, Victoria 8004, Australia. Correspondence e-mail: peter.lynch@csiro.au

High-brightness synchrotron X-rays together with precision achromatic focusing optics on beamline 7.3.3 at the Advanced Light Source have been applied for Laue microdiffraction analysis of mineralogical phases in Egyptian pigments. Although this task is usually performed using monochromatic X-ray diffraction, the Laue technique was both faster and more reliable for the present sample. In this approach, white-beam diffraction patterns are collected as the sample is raster scanned across the incident beam (0.8 mm \times 0.8 mm). The complex Laue diffraction patterns arising from illumination of multiple grains are indexed using the white-beam crystallographic software package XMAS, enabling a mineralogical map as a function of sample position. This methodology has been applied to determine the mineralogy of colour pigments taken from the ancient Egyptian coffin of Tjeseb, a priestess of the Apis bull dating from the Third Intermediate to Late period, 25th Dynasty to early 26th Dynasty (747 to 600 BC). For all pigments, a ground layer of calcite and quartz was identified. For the blue pigment, cuprorivaite ($\text{CuCaSi}_4\text{O}_{10}$) was found to be the primary colouring agent with a grain size ranging from 10 to 50 nm. In the green and yellow samples, malachite [$\text{Cu}_2(\text{OH})_2\text{CO}_3$] and goethite [$\text{FeO}(\text{OH})$] were identified, respectively. Grain sizes from these pigments were significantly smaller. It was possible to index some malachite grains up to 20 nm in size, while the majority of goethite grains displayed a nanocrystalline particle size. The inability to obtain a complete mineralogical map for goethite highlights the fact that the incident probe size is considerably larger than the grain size. This limit will continue to improve as the present trend is toward focusing optics approaching the diffraction limit (1000 \AA smaller beam area).

1. Introduction

Since its inception, X-ray diffraction (XRD) has provided a robust method for studying mineralogical associations in crystalline samples. For the majority of cases this is a relatively trivial task where the peak position and relative peak intensity provide a means to determine the mineralogy. It is widely understood that a number of well known sample characteristics exist which render conventional monochromatic XRD methods problematic. These include spotted ring patterns arising from large-grained samples, preferred orientation and peak overlap from highly heterogeneous and low-symmetry crystal structures. Moreover, physically small samples typically encountered in archeological studies limit the counting statistics necessary for phase identification due to the small volume of material diffracting at any time.

An alternate approach, particularly effective for small heterogeneous samples found in many archeological examples,

is white-beam X-ray microdiffraction (mXRD). Arising from the advent of high-brightness synchrotron sources, high-efficiency achromatic X-ray focusing optics and advanced computational indexing algorithms, white-beam mXRD represents a rapidly evolving field of X-ray diffraction. In addition, development of white-beam Laue diffraction offers several advantages for protein crystallography applications (Ren et al., 1999). A number of mXRD beamlines are in operation around the world, including the Advanced Light Source (ALS) and Advanced Photon Source (APS), while other stations are presently under construction. These facilities offer the ability to operate in either a white/pink-beam or monochromatic mode with sub-micrometre spatial resolution. Consequently, illuminating a sub-micrometre spot with high

flux is ideally suited for mineral identification from very small sample volumes. Furthermore, the high spatial resolution provides a method for obtaining a mineralogical map in materials that may exhibit a heterogeneous crystal structure.

For the case of white-beam μ XRD, microstructural information is obtained by recording the Laue pattern unique to an individual grain in a polycrystalline sample for a given energy bandpass. This methodology has been successfully employed to study a broad range of sample applications under various conditions. For example, an extensive amount of research has been used to study plastic deformation processes (Spolenak et al., 2003; Valek et al., 2003) and dislocation interactions (Barabash et al., 2001, 2003). A common feature of many of these studies is the uniform mineralogy of the sample, i.e. composed of a single mineralogical species or thin film deposited on a single-crystal substrate.

In cases when samples display a heterogeneous mineralogy, a monochromatic μ XRD approach has typically been applied to obtain mineralogical phase information; see for example Manceau et al. (2003). Mineralogical maps are obtained by integrating the intensity over a given diffraction ring for a series of patterns recorded as a function of (XY) position on the sample. For a highly focused incident beam, the reliability of this method is highly dependent upon the sampled grain size. The study of Gallo-Roman Terra Sigillata ceramics (Sciau et al., 2006) showed that reliable mineralogical mapping could be achieved when the average grain size (nanocrystalline) is significantly smaller than the X-ray beam. However, when the grain size increases beyond the nanocrystallite size, the non-uniform intensity distribution in the observed ring pattern renders the approach unreliable.

In contrast, white-beam μ XRD methods rely on the crystal structure and characteristic symmetry of the recorded Laue pattern to obtain grain mineralogy information. A drawback with this approach is the complex nature of the collected Laue pattern. For example, when multiple grains are illuminated or when several mineralogical phases are present, indexation is problematic. Recent advances in white-beam Laue methods can be attributed to the associated development of automated indexation software (Chung & Ice, 1999; Tamura et al., 2003). The ability to resolve the orientation matrix from more than ten overlapping grains makes mineralogical phase identification based on white-beam methods highly favourable. This approach was used to identify large quartz grains in Terra Sigillata ceramics (Sciau et al., 2006). Although presently restricted to micrometre-sized grains, it is anticipated that the demand for white-beam mineralogical identification methods will increase as current trends in X-ray focusing optics approach the diffraction limit. This will open up possibilities for the determination of phase information from nanoscale grain sized materials.

In the present study, the potential of Laue white-beam microdiffraction for mineralogical phase identification is addressed. As a demonstrative example, the methodology is applied to ancient Egyptian pigments. This sample was selected as previous monochromatic XRD data provided inconclusive evidence of the mineralogical speciation due to

restrictions on the physical size of the sample. After discussing experimental requirements for Laue data collection, the basis of the applied indexation methodology is discussed. Finally, mineralogical grain maps for each pigment are presented.

2. Experimental

In the National Gallery of Victoria (NGV), Australia, the conservation treatment of a deteriorated Egyptian inner anthropoid coffin is being undertaken. The coffin and mummy of Tjeseb, a priestess (probably about 17 years old) of the Apis bull, were among the first Egyptian antiquities to arrive in Australia in about 1890. They date to the Third Intermediate to Late period, 25th Dynasty to early 26th Dynasty (747-600 BC). The coffin is constructed from a wooden framework and covered with mud, then coated with fabric and a white pulverized ground layer acting as a support for the thin coloured paint layer used to decorate the coffin lid. It is heavily fragmented and several larger pieces exist (Fig. 1), along with hundreds of smaller dislocated flakes ranging in size from 2 to 15 mm. To determine the mineralogy of the paint pigments, μ XRD- μ XRF (X-ray fluorescence) measurements were performed on two flakes with blue, green and yellow pigments. Cross sections of the paint layer were



Figure 1

A portion of the front panel, typical of the decoration on the coffin lid. μ XRD- μ XRF data were collected from dislocated flakes containing blue, green and yellow pigments.

Table 1
The four high-intensity reflections, d spacings and Miller indices of the crystal structures for some of the minerals anticipated in the Egyptian pigments.

	Relative intensity I, hkl, d (Å)			
Cuprorivaite (CuCaSi ₄ O ₁₀)	100, 212, 3.00	96, 202, 3.29	79, 104, 3.36	62, 004, 3.78
Liebauite (Ca ₃ Cu ₅ Si ₉ O ₂₆)	100, 226, 2.41	88, 116, 3.00	63, 226, 2.46	52, 110, 7.13
Goethite [FeO(OH)]	100, 101, 4.20	72, 111, 2.44	45, 301, 2.69	40, 212, 1.72
Malachite (Cu ₂ OH ₂ CO ₃)	100, 203, 2.86			
	$\frac{1}{1}$	$\frac{6}{220}, \frac{3}{69}$	$\frac{60}{120}, \frac{505}{505}$	$\frac{52,020}{5,99}$

prepared by embedding the paint flakes (2 mm²) in epoxy resin. The sections were ground and polished to reveal a thin coloured paint layer above the white ground layer.

All experiments were performed on the high-resolution synchrotron X-ray microdiffraction beamline 7.3.3 at the Advanced Light Source. The beamline utilizes an orthogonal pair of Kirkpatrick-Baez (Kirkpatrick & Baez, 1948) mirrors to focus the white beam to a sub-micrometre spot (0.8 mm²) on the sample. Although two operating schemes are available, i.e. white beam or monochromatic, for the present study a white-beam setting was employed for mineralogical phase identification. Consequently no sample rotation is necessary to achieve the Bragg diffraction condition. For a detailed review of the beamline characteristics the reader is referred to MacDowell et al. (2001).

Based on this arrangement, the sample is mounted on high-precision translation stages used to raster-scan the sample across the incident beam. For each step, the diffracted signal is collected using a large-area CCD detector (MAR133). Each pigment was then translated across the beam in 5 mm steps, generating an XY mineralogical map from a specific region of interest. A total of three diffraction maps were collected, one for each pigment colour. In addition, based on mXRF, chemical information maps were produced from the same region of interest for each sample.

An important aspect of the beamline end-station, necessary for the present study, is the flexibility to change diffraction geometry in accordance with the sample mineralogy of interest. For the present study, identification of the pigment mineralogy relies on collecting high-intensity large-d-spacing reflections, minimizing the potential of peak overlap. Furthermore, to provide a direct comparison of the monochromatic and Laue diffraction data, without having to change the sample position, an asymmetric reflection geometry was employed with an incident beam to sample angle $\theta = 10^\circ$, and CCD detector to sample angle $2\theta = 60^\circ$. To highlight this point, Table 1 shows the four highest intensity reflections and respective d spacings for some of the minerals anticipated in the Egyptian pigments (Lee & Quirke, 2000).

3. Results

A critical aspect in microdiffraction studies is the grain-probe size relationship. For a monochromatic mXRD experiment, when the grain size exceeds the probe size, the number of grains contributing to the diffraction condition is reduced; consequently a continuous Debye-Scherrer ring pattern is no longer observed and/or the number of recorded reflections

may be limited. In these circumstances, phase identification is no longer reliable when a radial integration is performed across highly discontinuous ring patterns. In monochromatic studies, the nature of the grain-probe size problem in terms of subsequent mineral phase identification is addressed in the following.

The versatility of the beamline design (7.3.3 ALS) is apparent: by switching from monochromatic

to white beam, mXRD data were collected using a CCD area detector with mXRF data collected simultaneously using a SiLi detector from the same point on the sample. Monochromatic data collected for the blue pigment specimen are shown in Fig. 2. For all monochromatic data, incomplete Debye-Scherrer ring patterns were observed. Furthermore, the measured intensity from many single spots saturated the detector; consequently, counting times had to be reduced accordingly. Under these circumstances, radial integration along the 2θ direction (indicated in Fig. 2) to obtain X-ray peak intensity versus 2θ peak position data for phase identification is highly unreliable. To proceed under these conditions, only low-index (highly separated) discontinuous rings can be used with any degree of certainty. Fig. 2 shows the corresponding mineralogical match, given by indexation of the

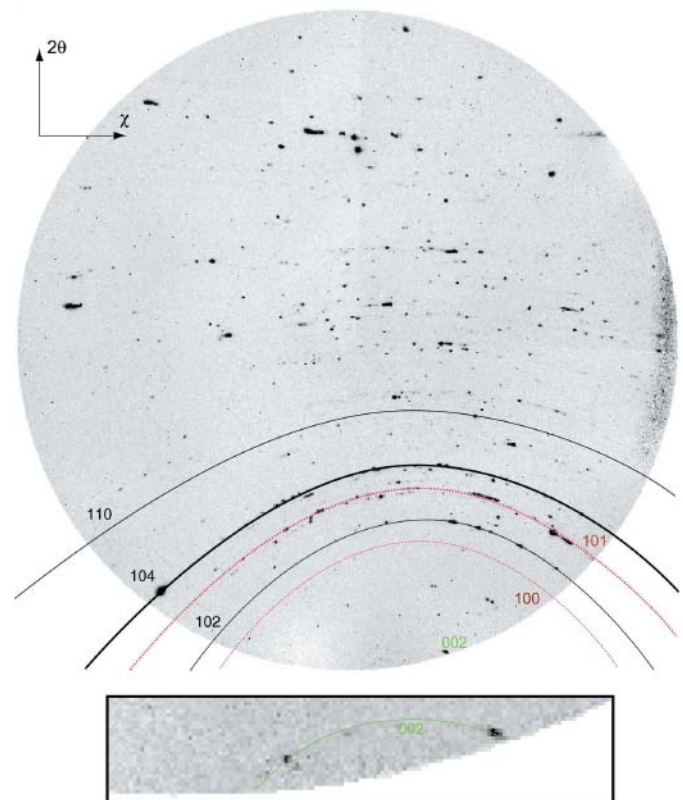


Figure 2
Monochromatic mXRD data ($\lambda = 2.07 \text{ \AA}$) collected for the blue pigment

sample showing the incomplete ring patterns of each mineralogical species. Miller indices for the low-angle reflections are given; black for calcite, red for quartz and green for cuprorivaite. Inset is a magnified region from the two-dimensional detector where individual spots were observed at $15.7^\circ 2\theta$, which may be attributed to the 002 reflection of cuprorivaite.

monochromatic ring pattern for calcite (black lines) and quartz (dotted red lines). However, traces of cuprorivaite were not apparent. In addition to monochromatic diffraction data, mXRF maps were recorded. In this case significant concentrations of Cu and Ca were observed. The presence of calcium and copper in the blue areas of the sample are consistent with the use of Egyptian blue (cuprorivaite, $\text{CuCaSi}_4\text{O}_{10}$) and its widespread use as a blue pigment at the time the coffin was constructed (Jaksch et al., 1983). Upon further inspection, some of the monochromatic diffraction data displayed several individual diffraction spots at low 2θ angles. The inset in Fig. 2 is a magnified region from the CCD image showing two individual spots at $15.7^\circ 2\theta$ ($d = 2.07 \text{ \AA}$) corresponding to the

002 reflection for cuprorivaite. Although this result represents a possible mineralogical match, the reliability of this approach could be flawed by the limited diffraction information collected using monochromatic radiation. It should be noted that the problem of large grain relative to beam size was encountered with all the samples. In an attempt to resolve this ambiguity and test for the presence of other mineral species, mineralogical phase identification using white-beam diffraction measurements was pursued.

Utilizing the wide bandpass and achromatic focusing optics, white-beam mXRD data were collected for all pigments. A pattern collected for the blue pigment is given in Fig. 3. The complex Laue pattern shown demonstrates that multiple grains are illuminated. Furthermore, from inspection of individual Laue spots, the distinctly different size, shape and observed intensity indicates that the Laue pattern is made of grains with a broad range of sizes, which may be attributed to

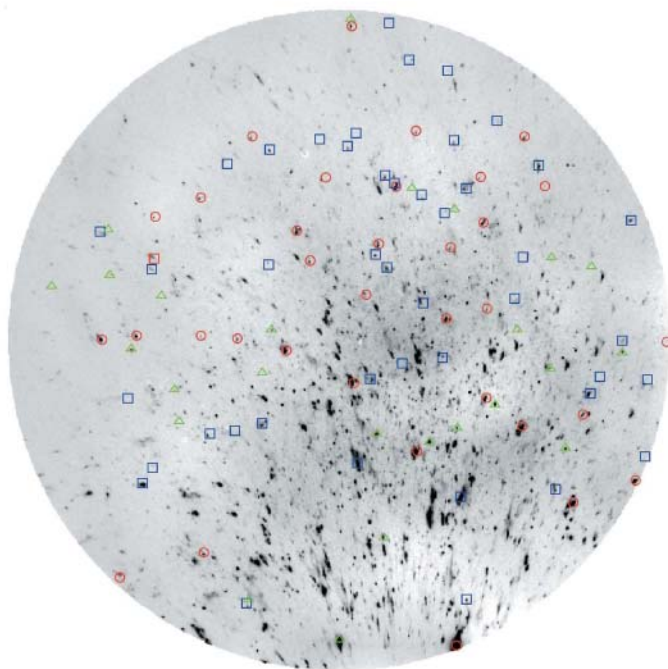


Figure 3
Illustrative example showing the complex nature of the white-beam data collected for the blue pigment specimen. Indexed Laue reflections are included for calcite (blue squares), quartz (red circles) and cuprorivaite (green triangles).

different mineralogical species. For example, the large black (high-intensity) Laue reflections arise from large 'slab-like' calcite grains contained in the ground layer. The underlying success of the white-beam methodology is the ability to index the observed complex Laue patterns; an overview of this procedure is given in the following section.

4. White-beam pattern indexation

All white-beam patterns were indexed using the mXRD software package X-ray Microdiffraction Analysis Software (XMAS).¹ To provide an overview of the indexation procedure, key steps in the routine are summarized below, while a more complete description is given by Tamura et al. (2003). For each CCD diffraction image, the collected pattern must be indexed according to hkl Miller notation. To perform this task, image-intensity peak positions from the CCD are automatically found using a peak-search routine. Once the peak positions are established, a subset of the most intense reflections is first considered. Based on the instrumental geometry calibration described below, the direction of the incident beam and position of the illuminated area on the sample are known relative to the CCD camera position. Combining information from the experimental geometry and fitted peak positions, directions of the experimental scattering vectors can be determined. Angles between these experimental scattering vectors are tabulated and compared with a 'reference' list of angles from the theoretical scattering vectors evaluated for the crystallite structure of interest and the energy bandpass of the polychromatic beam. The routine searches for angular matches between triplets of reflections within an adjustable angular tolerance parameter. Each triplet and corresponding hkl indices are then used to calculate a trial matrix with a complete list of reflections that should be visible on the CCD for the considered energy bandpass, CCD dimensions and experimental data collection geometry. The best match is the triplet that is able to index the largest number of experimental reflections.

The indexation process requires precise knowledge of the instrumental geometry. For calibration of the experimental configuration, typically a white-beam pattern from a 'strain-free' single crystal is collected. In this case, an Si wafer mounted adjacent to the sample is used. Prior to indexation, known experimental conditions are required as input parameters. The values of interest include: active area of CCD detector, 133 mm; angle of incident beam relative to the sample surface, $\theta = 10^\circ$, and angle of sample to CCD, $2\theta = 60^\circ$; white-beam energy bandpass, 5 to 15 keV; sample-to-detector distance, $d = 56 \text{ mm}$, and centre position of the CCD in the x direction, $X_{\text{cent}} = 630$ pixels, and in the y direction, $Y_{\text{cent}} = 550$ pixels. After successfully indexing the reference pattern, an iterative process based on linear least-squares refinement

¹XMAS is a software suite designed specifically for the analysis of X-ray microdiffraction data collected on beamline 7.3.3 at the Advanced Light Source (ALS). The software can be freely downloaded from the ALS microdiffraction website (http://xraysweb.lbl.gov/microdif/XMAS_download.htm).

is used to obtain a precise measure of the experimental geometrical parameters listed above. Making use of the calcite ground layer from each sample, a further refinement was possible: via refinement of the instrumental parameters from the calcite base, any errors which may be introduced from the irregular surface height of the samples were avoided.

In the present study, pattern indexation is based on a priori knowledge of the crystal structure. That is, a crystal structure, for example cuprorivaite, is entered as an input parameter and the presence of the material is defined by the ability to index each white-beam pattern successfully. The automated software routine repeats this process for every pattern in a given data set, creating a mineralogical map as a function of position on the sample. This is a very time-consuming process as many mineralogical phases must be tested. To speed up this process, possible mineralogical matches identified from monochromatic mXRD data, elemental information gained from mXRF data and previous literature studies undertaken on Egyptian pigments (see for example Lee & Quirke, 2000), were used to establish a 'trial list' of species to be tested for each pigment. For example, crystal structures tested for the blue pigment sample include cuprorivaite, liebauite, wollastonite, calcite and quartz. A white-beam pattern collected for the blue pigment is given in Fig. 3. From the list, indexed Laue patterns arising from single grains of calcite (blue squares), quartz (red circles) and cuprorivaite (green triangles) are indicated.

5. Analysis

Upon indexation of all recorded Laue patterns, the mineralogical heterogeneity of each sample can be represented by a two-dimensional grain map, specific to a particular mineral species. In each map individual grains are represented by the out-of-plane normal calculated from the orientation-matrix data. In this instance, two-dimensional grain size information is displayed by assigning a shade colour to the out-of-plane normal value. For the blue pigment sample, three maps are given in Fig. 4, showing the grain distribution for cuprorivaite (Fig. 4a), quartz (Fig. 4b) and calcite (Fig. 4c). Although retrieval of grain depth information was not undertaken, optical images indicate that the blue cuprorivaite pigment is on a white ground layer, presumably comprised of calcite and quartz. Measured grain sizes were found to be highly dependent on the mineral species. For the base layer, practically all of the mapped region was made up of large calcite grains, $\sim 100 \text{ mm}^2$ in size, whereas localized quartz grains, about 30 mm^2 , were found. For the blue pigment layer, cuprorivaite grains ranging in size from 10 mm^2 to 50 mm^2 were observed.

As a further reliability test of the white-beam methodology, a mXRD map was collected for a cross-section sample which included a yellow-green pigment interface. Elemental information was first obtained by recording a mXRF map about the interface. The elemental concentration of calcium, copper and iron was recorded as a function of position. Concentration changes of the three elements are illustrated in Fig. 5. Calcium levels remained fairly uniform as anticipated for the underlying calcite base layer. An increase in the calcium content at

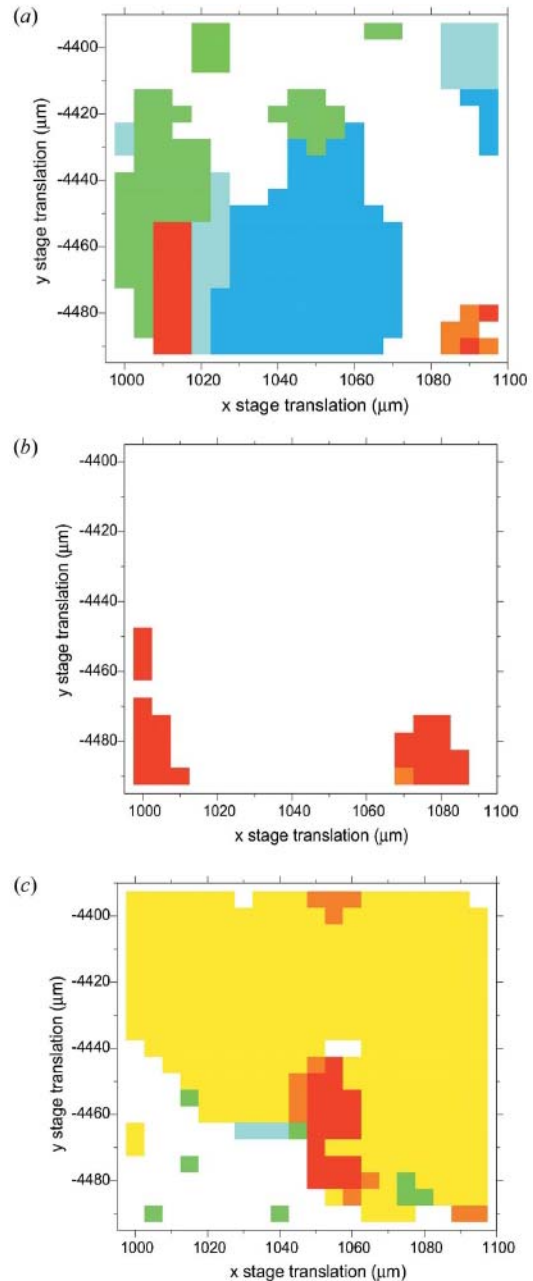


Figure 4
mXRD maps showing individual grains of each identified mineral species in the blue pigment sample: (a) cuprorivaite grain map; (b) quartz grain map; (c) calcite grain map. The distinctly different colour representations used in maps (a)-(c) highlight the characteristic orientation of each individual grain, while blank regions signify areas where no grains of a given species are observed.

the top of the map (Fig. 5c) can be attributed to the exposed calcite face in the cross section. In addition, a pronounced change in the copper and iron levels was observed at the yellow-green interface. The copper concentration was greatest in the green pigment; similarly the iron concentration was highest in the yellow pigment. It is anticipated from the change in elemental data an equivalent mineralogical change should be observed from the different colouring pigments.

For the yellow-green pigment interface, mXRD grain maps are given in Fig. 6, showing the distribution of calcite (Fig. 6a),

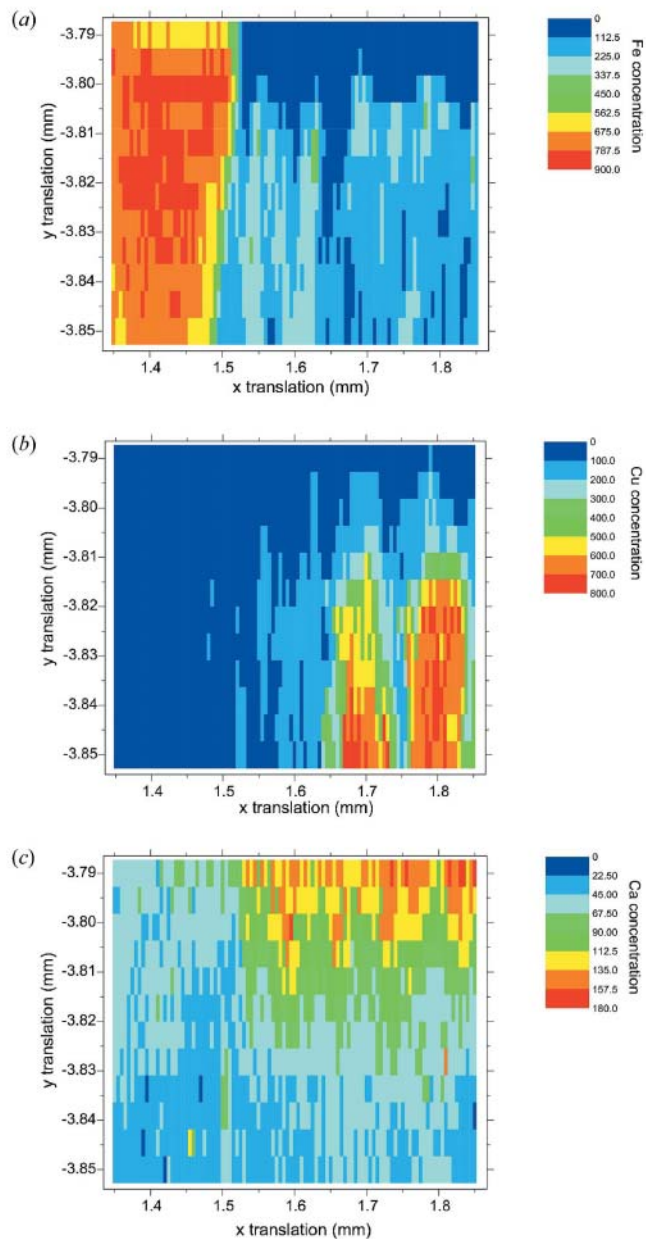


Figure 5
mXRF maps showing elemental concentration changes across the yellow- green pigment interface: (a) iron elemental concentration; (b) copper elemental concentration; (c) calcium elemental concentration.

quartz (Fig. 6b) and malachite (Fig. 6c). Similar to the blue pigment sample, large calcite grains (up to 100 mm^2) and a number of quartz grains of about 30 mm^2 in size were observed. In Fig. 6(c) the majority of malachite grains are 20 mm , for example.

Mineralogy of the yellow pigment could not be established using white-beam methodology. As the availability of synchrotron beam time was limited, monochromatic mXRD data obtained from a laboratory source, shown in Fig. 7, were used to establish goethite as the predominant mineral species in the yellow pigment. From Fig. 7, the continuous nature of the weakly diffracting Debye-Scherrer rings observed for the 110, 130 and 111 goethite reflections, and the associated line

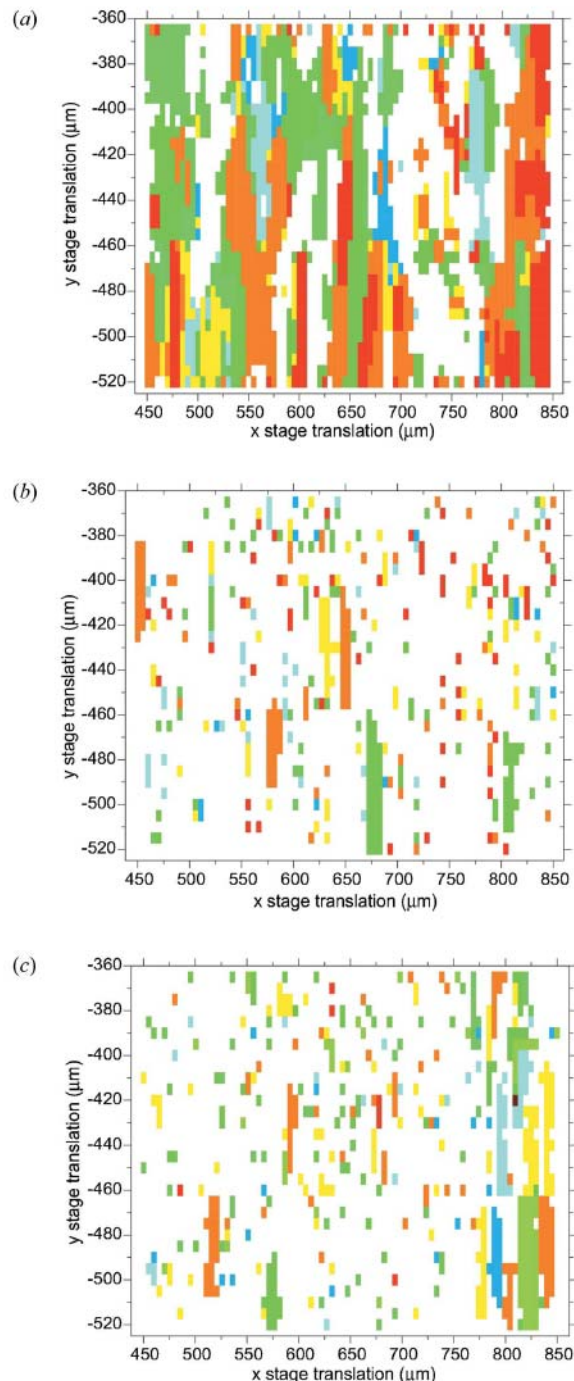


Figure 6
mXRD maps showing individual grains of each identified mineral species in the yellow-green pigment interface: (a) calcite grain map; (b) quartz grain map; (c) malachite grain map. The distinctly different colour representations used in maps (a)-(c) highlight the characteristic orientation of each individual grain, while blank regions signify areas where no grains of a given species are observed.

broadening, is indicative of a nanocrystalline grain structure. In this instance, the line broadening of goethite can be more easily identified by integration along 2θ , as shown in Fig. 7(b). The inability to detect goethite from white-beam measurements can be attributed to a nanocrystalline grain structure, i.e. the grain size is significantly smaller than the 1 mm synchrotron probe size.

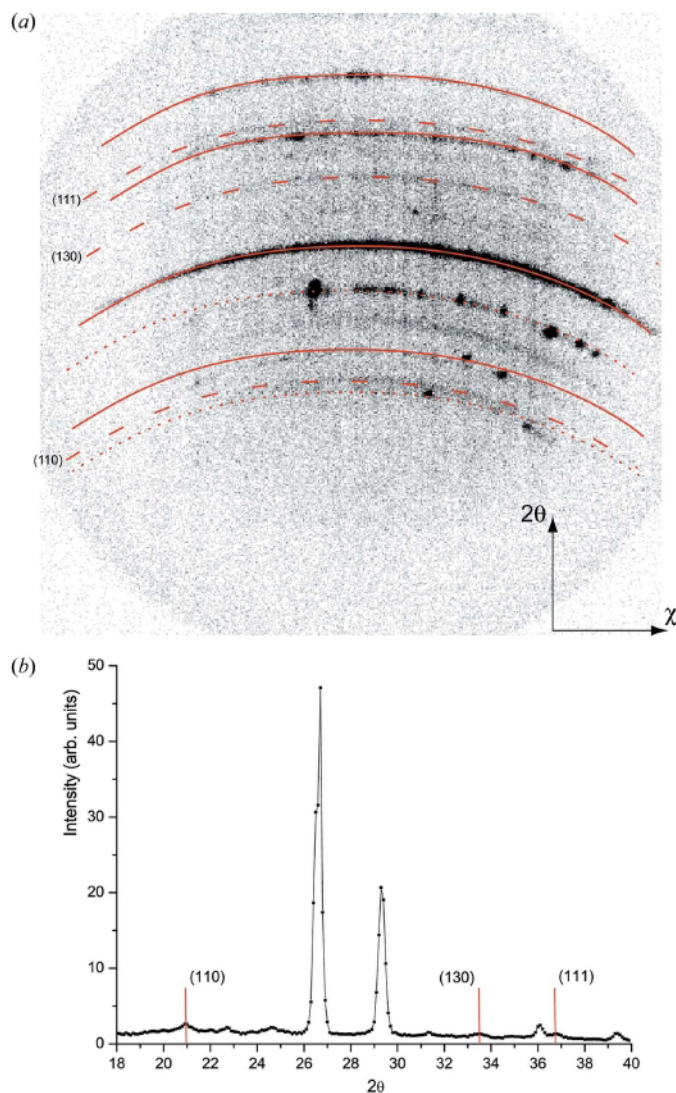


Figure 7 Monochromatic mXRD data collected from a laboratory instrument in the yellow pigment region. (a) Indexation of calcite and quartz are identified by the solid and dotted lines, respectively, while dashed lines highlight the diffuse rings from the goethite (yellow) pigment. (b) Radial integration (range from 2θ to 0°) of the monochromatic data highlighting the broad low-intensity goethite peaks.

A feature identified by the number of randomly distributed single-step blocks in the mXRD grain maps (Figs. 6b and 6c) in the malachite and to a lesser extent the quartz arises as grain sizes approach the lower limit of applicability of the white-beam method, defined when the grain size is equal or less than the incident probe size. Although not tested specifically in this study, this lower limit can be defined as the ability to index a single white-beam diffraction pattern unambiguously. Although this can be ascertained from the fit achieved for a diffraction pattern, the ability to obtain the same indexation result for consecutive raster scan step increments reinforces the credibility of the initial indexation result. Consequently, the step increment, in this work 5 μm , can be considered as an estimate of the minimum grain size probed for this set of experimental data. Furthermore, another implication of the probe size observed in the diffraction maps is the false elon-

gation of the grain size in the y direction, arising from the extended beam footprint on the sample in the y direction due to the collection angle $\Delta = 10^\circ$. For a 0.8 mm probe size, the $x:y$ aspect ratio of the beam footprint on the sample is 1:6.

6. Discussion

Realisation of spatially resolved mineralogical data represents information that has only recently been achieved through the development of efficient focusing optics and high-brightness synchrotron sources. The underlying benefit of this approach is evident in the study of samples that exhibit a complex heterogeneous mineralogy which may be difficult to resolve using conventional powder diffraction techniques and in circumstances where the mineralogy changes throughout the sample. In addition, the non-destructive nature of X-ray diffraction is well suited for the study of artwork and precious artefacts which demand non-destructive analytical methodologies for art authentication, attribution and provenance assessment.

Continued development of white-beam mineralogical phase identification methodology, demonstrated in this article, displays a number of benefits in comparison with standard monochromatic microdiffraction methods. The increased flux available using a white beam leads to a significant reduction in counting times. For example, in the present study, counting times could be reduced by a factor of about 10^4 with respect to monochromatic data collection. Furthermore, white-beam methods provide additional information, including grain orientation, not directly achieved with monochromatic methods.

It is anticipated that further advances in white-beam mineral identification will be realised in the near future. Potential improvements are linked to the development of high-efficiency achromatic focusing optics and increased flux of the X-ray source. Based on a Kirkpatrick-Baez arrangement, focal spots of 50 nm (Mimura et al., 2005) and 90 nm (Hignette et al., 2005) have recently been reported. Although present white-beam methods are restricted to grain sizes greater than a micrometre, nanometre focusing will reduce this grain size limitation to the sub-micrometre scale. Such improvements will be possible in time at white-beam micro-diffraction end-stations supporting nanometre focusing.

7. Conclusion

Utilizing a highly focused white beam, Laue microdiffraction methods have proven successful in determining the mineralogy of colouring pigments taken from an ancient Egyptian coffin of Tjeseb, a priestess of the Apis bull dating to the Third Intermediate to Late period, 25th Dynasty to early 26th Dynasty (747 to 600 BC). The merits of the white-beam methodology for mineralogical phase identification have been demonstrated for two colour pigments. For the blue pigment, cuprorivaite ($\text{CuCaSi}_4\text{O}_{10}$) was found to be the primary colouring agent with a grain size ranging from 10 to 50 μm . In the green-yellow cross section, malachite [$\text{Cu}_2(\text{OH})_2\text{CO}_3$]

and goethite [FeO(OH)] were identified, respectively. It was possible to index some malachite grains up to 20 nm in size, while the majority of goethite grains displayed a nanocrystalline particle size which required monochromatic techniques for phase identification. The identification of pigments on the coffin contributes to the body of knowledge pertaining to colouring materials used in ancient Egyptian funeral objects. Knowledge specific to this artefact will guide conservation treatments on the coffin and inform decisions regarding storage and display. Furthermore, present limitations and future prospects arising from the grain-probe size relationship have been addressed. It is anticipated that the potential of white-beam methodology will be further enhanced with nanometre-scale X-ray probe sizes.

This work was supported by the Victorian Centre for Advanced Materials Manufacturing (VCAMM). The Advanced Light Source is supported by the Director, Office of Science, Office of Basic Energy Sciences, of the US Department of Energy under Contract No. DE-AC02-05CH11231.

References

- Barabash, R. I., Ice, G. E., Larson, B. C., Pharr, G. M., Chung, K.-S. & Yang, W. (2001). *Appl. Phys. Lett.* 79, 749-751.
- Barabash, R. I., Ice, G. E., Tamura, N., Valek, B. C., Bravman, J. C., Spolenak, R. & Patel, J. R. (2003). *J. Appl. Phys.* 93, 5701-5706.
- Chung, J.-S. & Ice, G. E. (1999). *J. Appl. Phys.* 86, 5249-5255.
- Hignette, O., Cloetens, P., Rostaing, G., Bernard, P. & Morawe, C. (2005). *Rev. Sci. Instrum.* 76, 63709(1-5).
- Jaksch, H., Seipel, W., Weiner, K. L. & Goresy, A. E. (1983). *Naturwissenschaften*, 70, 525-535.
- Kirkpatrick, P. & Baez, A. V. (1948). *J. Opt. Soc. Am.* 38, 766-774.
- Lee, L. & Quirke, S. (2000). *Ancient Egyptian Materials and Technology*. Cambridge University Press.
- MacDowell, A. A., Celestre, R. S., Tamura, N., Spolenak, R., Valek, B. C., Brown, W. L., Bravman, J. C., Padmore, H. A., Batterman, B. W. & Patel, J. R. (2001). *Nucl. Instrum. Methods Phys. Res. A*, 467-468, 936-943.
- Manceau, A., Tamura, N., Celestre, R. S., MacDowell, A. A., Geoffroy, N., Sposito, G. & Padmore, H. A. (2003). *Environ. Sci. Technol.* 37, 75-80.
- Mimura, H., Matsuyama, S., Yumoto, H., Hara, H., Yamamura, K., Sano, Y., Shibahara, M., Endo, K., Mori, Y., Nishino, Y., Tamasaku, K., Yabashi, M., Ishikawa, T. & Yamauchi, K. (2005). *Jpn J. Appl. Phys.* 44, L539-L542.
- Ren, Z., Bourgeois, D., Helliwell, J. R., Moffat, K., Srajer, V. & Stoddard, B. L. (1999). *J. Synchrotron Rad.* 6, 891-917.
- Sciau, P., Goudeau, P., Tamura, N. & Dooryhee, E. (2006). *Appl. Phys. A*, 83, 219-224.
- Spolenak, R., Brown, W. L., Tamura, N., MacDowell, A. A., Celestre, R. S., Padmore, H. A., Valek, B., Bravman, J. C., Marieb, T., Fujimoto, H., Batterman, B. W. & Patel, J. R. (2003). *Phys. Rev. Lett.* 90, 96102(1-4).
- Tamura, N., MacDowell, A. A., Spolenak, R., Valek, B. C., Bravman, J. C., Brown, W. L., Celestre, R. S., Padmore, H. A., Batterman, B. W. & Patel, J. R. (2003). *J. Synchrotron Rad.* 10, 137-143.
- Valek, B. C., Tamura, N., Spolenak, R., Caldwell, W. A., MacDowell, A. A., Celestre, R. S., Padmore, H. A., Bravman, J. C., Batterman, B. W., Nix, W. D. & Patel, J. R. (2003). *J. Appl. Phys.* 94, 3757-3761.